HHS Public Access

Author manuscript

J Surg Res. Author manuscript; available in PMC 2019 December 01.

Published in final edited form as:

J Surg Res. 2018 December ; 232: 570–577. doi:10.1016/j.jss.2018.07.015.

Tracking macrophage infiltration in a mouse model of pancreas cancer with the PET tracer [11C]PBR28

Mirna Perusina Lanfranca[a], **Jenny Lazarus**[a], **Xia Shao**[b], **Hari Nathan**[a], **Marina Pasca Di Magliano**[a], **Weiping Zou**[a], **Morand Piert**[b], and **Timothy L. Frankel**[a]

[a]Department of Surgery, University of Michigan, 1500 East Medical Center Drive, Ann Arbor, MI, USA 48109

[b]Department of Radiology, University of Michigan, 1500 East Medical Center Drive, Ann Arbor, MI, USA 48109

Abstract

Background: The tumor microenvironment of pancreatic ductal adenocarcinoma (PDAC) contains abundant immunosuppressive tumor associated macrophages (TAM). High level of infiltration is associated with poor outcome and is thought to represent a major roadblock to lymphocyte based immunotherapy. Efforts to block macrophage infiltration has been met with some success but non-invasive means to track TAMs in PDAC are lacking. Translocator protein (TSPO) is a mitochondrial membrane receptor which is upregulated in activated macrophages. We sought to identify if a radiotracer labeled cognate ligand could track macrophages in PDAC.

Materials and Methods: A murine PDAC cell line was established from a transgenic mouse with pancreas specific mutations in KRAS and the p53. After confirming lack of endogenous TSPO expression, tumors were established in syngeneic mice. A radiolabeled TSPO specific ligand ([11C]PBR28) was delivered intravenously and tumor uptake assessed by autoradiography, ex vivo, or micro-PET imaging.

Results: Resected tumors contained abundant macrophages as determined by immunohistochemistry and flow cytometry. Immunoblotting revealed murine macrophages expressed TSPO with increasing concentration on activation and polarization. Autoradiography of resected tumors confirmed [11C]PBR28 uptake and whole mount sections demonstrated the ability to localize tumors. To confirm the findings were macrophage specific, experiments were

Correspondence: Timothy L. Frankel, MD, 1500 East Medical Center Dr, Ann Arbor, MI 48109, timofran@med.umich.edu, ph: 734-936-7607, fx: 734-232-6188.

Author contributions: Each author listed made a significant contribution to the study presented. MPL is the lead author and performed many of the experiments and wrote the manuscript. JL and YZ assisted in experimental tasks and wrote portions of the paper. XS and PS assisted in the animal studies and generation of the nucleotide as well as review of the manuscript. MPM, WZ, MP and TLF proposed the experimental design and helped construct and edit the final manuscript.

Disclosures: Authors report no financial and/or personal relationships with other people or organizations that could potentially and inappropriately influence (bias) this work and conclusions.

repeated in CD11b deficient mice and the radiotracer uptake was diminished. Micro-PET imaging validated radiotracer uptake and tumor localization in a clinically applicable manner.

Conclusion: As new immunotherapeutics reshape the PDAC microenvironment, tools are needed to better measure and track immune cell subsets. We have demonstrated the potential to measure changes in macrophage infiltration in PDAC using [11C]PBR28.

Keywords

Pancreatic Cancer; Tumor Associated Macrophages; PET imaging

Introduction

Pancreatic ductal adenocarcinoma (PDAC) is a near universally fatal disease with a 5 year survival of 9%(1, 2). While cancers such as melanoma, renal cell carcinoma and non-small cell lung cancer appear relatively sensitive to cytotoxic T-cell based checkpoint inhibition, PDAC has been resistant(3). In trials of both anti-CTLA-4(4) and PDL-1 antibodies(5) there have been few if any responders and no durable cures. Recent progress targeting myeloid cells has been met with some success, as prevention of macrophage trafficking to tumors appears to improve response to chemotherapy(6–8). Macrophage mobilization from the bone marrow to PDAC tumors is an independent predictor of poor survival after surgical resection(7). Given the important implications in prognosis and cancer treatment, non-invasive methods to measure and track macrophage infiltration into tumors are needed.

Translocator protein (TSPO) (previously called peripheral benzodiazepine receptor (PBR)) is an 18kDA, five transmembrane domain protein located on the mitochondrial membrane and primarily involved in cholesterol transport and steroid synthesis(9, 10). TSPO is present at low levels in all tissues including the brain, where it is currently being studied as a marker for neural inflammation(11, 12). It has been established that during activation, microglial cells, like all phagocytic cells(13), express binding sites for TSPO allowing them to be targets for novel radiotracer labeled compounds.

[11C]PBR28 is a Carbon-11 radiolabeled high-affinity ligand for TSPO developed for Positron Emission Tomography (PET) of subtle brain inflammation seen in conditions such as Parkinson’s Disease(12), Alzheimer’s and stroke(14). Biodistribution studies identified high levels of [11C]PBR28 binding in heart, lung and kidney tissues and relatively low levels in brain, intestine and pancreas(13). Previously, our group determined that [11C]PBR28 could also be used to identify extra-neuroaxial sites of inflammation related to experimentally induced aortic aneurysms and arthritis (15, 16). Here, the [11C]PBR28 uptake was directly proportional to macrophage infiltration and *in vitro* studies confirmed rapid uptake of radiotracer by macrophages on activation. We sought to determine if macrophage recruitment to pancreas cancer could be identified using [11C]PBR28 small animal PET.

Materials and Methods

Radiotracer synthesis

[11C]PBR28 was synthesized using modified GE Tracerlab FX C Pro based on the method describe by Shao et al. (17). Briefly, after dissolving the precursor, desmethylPBR28 TBA salt (1 mg) was dissolved into absolute ethanol (100 ¼L), it was loaded onto the 2 mL stainless steel HPLC loop, and conditioned with nitrogen gas for 20 seconds at 10 mL/min. [11C]MeOTf was prepared according to the general procedure and passed through the HPLC loop at 12 mL/min for 5 minutes. Following reaction, the mixture was purified by semi-preparative HPLC (column: Luna C5 100×10 mm, mobile phase: 20 mM ammonium acetate in 40% ethanol, flow rate: 3 mL/min). The radioactive product peak was collected (retention time ~10 min) into 25 mL of water and then passed through a C-18 extraction cartridge. The cartridge was washed with 5 mL USP water. The final product was eluted with 0.5 mL of USP ethanol, followed by 9.5 mL of USP saline for injection. The aqueous solution was filtered through a 0.22 ¼m sterile filter into a sterile dose vial and submitted for QC testing. Quality control analyses were performed according to guidelines outlined in chapter 823 of the US Pharmacopeia and previous reported.

Mouse models

All animal studies were conducted in compliance and with approval of the University of Michigan Committee on Use and Care of Animal. Males and females were used with equal frequency and without special consideration. To study macrophage infiltration, subcutaneous implantation of an established murine PDAC cell line into syngeneic mice was utilized. The cell line 4668 possesses a p48 driven tetracycline inducible KRAS G12D mutation with a heterozygous mutated p53 (p48Cre;TetO-KrasG12D; Rosa26rtTa/+; p53R172H/+)(18). In the presence of doxycycline, cells demonstrate increased proliferation and form tumors that histologically mirror the PDAC from which they were derived. Cells were maintained in RPMI supplemented with 10% fetal bovine serum and 1 ¼g/ml of doxycycline to maintain KRAS activation. At the time of implantation, 2×10^6 cells were injected into each flank of mice which were monitored daily. Doxycycline was administered in the drinking water at a concentration of 0.2 g/l in a solution of 5% sucrose and replaced every 3–4 days(18). CD11b-DTR mice (B6.FVBTg (ITGAM-DTR/EGFP)34Lan/J, Jackson Laboratory) were administered diphtheria toxin (DT) i.p. at a dose of 25 ng/g every 4 days as previously described(19). At two weeks, mice were sacrificed and tumors excised and processed for histology or flow cytometry.

Immunoblotting

Tissue fragments were mechanically disrupted and placed in ice cold RIPA lysis and extraction buffer (Thermo) supplemented with protease inhibitors (Halt™ Protease and Phosphatase Inhibitor Cocktail, Thermo Scientific™). After incubation samples were centrifuged and the supernatant fraction was removed and protein concentration measured using BCA colorimetric assay (Invitrogen) per manufacturer's instructions. Equal quantity of protein was loaded onto 12% polyacrylamide gels and then electrotransferred to polyvinylidene difluoride membranes at 100V for 60 minutes. Membranes were blocked with 5% milk (Blotto, Santa Cruz sc-2325) in TBS-T (tris-buffered saline (TBS) Tween20)

for 60 minutes and then incubated overnight at 4 °C with antibodies directed against TSPO (EPBR5384, Abcam 109497) or GAPDH (cell signaling, 5174S). After washing and application of an HRP conjugated secondary antibody, blots were exposed with enhanced chemiluminescent (ECL, Pierce) substrate detected by autoradiography.

Macrophage separation and polarization

To assess for TSPO in macrophages, splenocytes were harvested from B7/C56 mice and processed to single cell suspension. Macrophages were separated using F4/80 microbeads (Miltenyi Biotec) per the manufacturer's protocol. To polarize macrophages to an M1 phenotype, sorted cells were cultured in the presence of LPS (50ng/mL) for 48 hours. For M2 macrophages, sorted cells were cultured in media containing 20 ng/ml of IL-4 and 20 ng/ml of IL-10. Polarization was confirmed by flow cytometry staining for arginase and iNOS.

Histology and Immunohistochemistry

Tumor and normal tissues were fixed in formalin and paraffin embedded (FFPE) or flash frozen in OCT and stained with hematoxylin and eosin (H&E). Immunohistochemistry was performed using antibodies directed against F4/80 (1:100; BMA biomedical) and TSPO (1:200, Abcam). Photographs were taken using an Olympus BX-51 microscope with an Olympus DP71 digital camera.

Flow cytometry

After excision, fresh spleens and tumors were processed to single cell suspension by mechanical disruption and passage through 40¼m filters. After serial washing in MACS buffer (Phosphate-buffered saline (PBS)+2% FBS+ 1mM EDTA), cells were stained with antibodies to CD45(BD Biosciences), CD3(BD Biosciences), F4/80(AbDSerotec), and CD11b (BD Biosciences). Flow cytometric analysis was performed on an LSR II (BD) and data were analyzed with FACSDIVA software (BD Biosciences).

Autoradiography and PET imaging

Bilateral flank tumors were established in wild type or CD11b-DTR mice, as described. For autoradiography, at two weeks, mice were anesthetized and intravenously injected with on average 79.6 (range 40 – 112) MBq of [11C]PBR28 (in 0.2 mL). After 20 minutes, mice were sacrificed and tumors, kidney (positive control) and skeletal muscle (negative control) were harvested and flash frozen in OCT. For cross-sectional (whole body) mounts, mice were euthanized and placed at −80°C for 20 minutes. Axial sections encompassing the flank tumor were obtained and placed in OCT.

In-vivo PET imagining was performed after intravenous tail vein injection of on average 35 MBq of [11C]PBR28, followed by a 60 minute dynamic scan on a P4 micro-PET scanner (Concorde/Siemens, Knoxville, TN). Subcutaneous tumors were placed in the region of the chest to capture the cardiac blood pool and limit interference from the spleen and kidneys.

Statistics

Nominal variables were evaluated using 2-tailed $\chi 2$ or Fisher's exact tests as appropriate. Continuous variables were assessed by univariate logistic regression for parametric values and Wilcoxon rank sum for nonparametric values. A p-value < 0.05 was considered significant.

Results

The tumor microenvironment of pancreatic cancer contains abundant macrophages

To evaluate the immune infiltration in subcutaneously implanted pancreatic tumors, a PDAC cell line (4668) was established from the pancreas of a p48Cre;TetO-KrasG12D; Rosa26rtTa/+; p53R172H/+ transgenic mouse with histologically proven PDAC. After placement into the flanks of mice they were allowed to grow in the presence of doxycycline for two weeks. At excision, IHC revealed a dense infiltration of F4/80 positive cells characteristic of macrophages (Figure 1a). There were slightly more cells seen at the peripheral edges of tumors compared to the center. After processing tumors to a single cell suspension, flow cytometry analysis identified 48% of infiltrating immune cells as $CD45^+$, $CD11b^+$, $F4/80^+$ confirming macrophage infiltration (Figure 1b). CD11bDTR mice possess a diphtheria toxin receptor transgene in myeloid cells which results in lethal sensitivity of macrophages to DT(19). After three doses of DT, IHC confirmed a dramatic reduction in tumor infiltrating macrophages when compared to untreated mice (Figure 1c,d).

Macrophages and not pancreatic cancer cells express TSPO

To determine if pancreatic cancer cells express TSPO the PDAC line 4668 was cultured with and without doxycycline which is required for KRAS mutation and activation. Immunoblot performed against TSPO revealed undetectable levels of the protein in KRAS active and inactive PDAC cells (Figure 2a). To confirm TSPO presence in macrophages, protein lysates were obtained from fresh splenocytes as well as sorted macrophages (Figure 2a,b). There was abundant TSPO in splenocytes and macrophages which increased in M1 and M2 polarizing conditions (Figure 2b). To confirm in vitro findings, immunofluorescent staining was performed on subcutaneously established PDAC tumors. Staining confirmed that TSPO was present in macrophages but not in pancreatic epithelial cells, lymphocytes or fibroblasts (Figure 2c-f).

Macrophage rich tissues take up radiotracer [11C]PBR28

Autoradiography performed on extracted tissues after [11C]PBR28 injection revealed abundant radiotracer uptake in pancreatic tumors (Figure 3a,b). Positive and negative controls included kidney, which is known to contain abundant TSPO, and normal muscle which does not and contains virtually no immune infiltrate. To determine if the uptake in pancreatic tumors was macrophage specific, tumors were established in CD11b-DTR mice and subjected to identical radiotracer injection after one week of DT treatment. Autoradiography confirmed that pancreatic tumors lacking macrophages had significantly less [11C]PBR28 radiotracer uptake (Figure 3a,b) and were similar in intensity to muscle (Figure 3c,d).

Sections of the same tissues used for autoradiography were subjected to immunofluorescent staining with antibodies directed against TSPO and F4/80. This confirmed both macrophage infiltration in the subcutaneous tumors and TSPO distribution in muscle and kidney tissues (Figure 4a-c).

[11C]PBR28 can localize pancreatic tumors in mice

To determine if [11C]PBR28 could be used to localize macrophage rich tumors, whole mount cross sections of mice bearing implanted tumors were prepared (Figure 4d). Autoradiography confirmed that peripheral uptake of tumors was readily visible with minimal staining in the neutrophil rich necrotic center (Figure 4e). To confirm these results in vivo, mice were injected with [11C]PBR28 and underwent microPET imaging. In three tested mice, tumors were easily identified on axial and coronal imaging. A representative example is displayed (Figure 5).

Discussion

Pancreatic ductal adenocarcinoma incidence continues to rise and is currently the third leading cause of cancer related deaths in the United States(2). It is among the most lethal malignancies with an estimated 5-year survival of only 9%(20). Unlike breast and colon cancer in which the development of new chemotherapeutic and targeted therapies has translated into improved survival, the mortality from PDAC has remained unchanged for decades(21). The advent of lymphocyte modulators and checkpoint inhibitors have provided durable responses to previously difficult to treat malignancies such as non-small cell lung cancer, but has had little impact on PDAC(4, 5). One proposed mechanism for this relative resistance is the dense infiltration of suppressive myeloid cells characteristic of PDAC, such as myeloid derived suppressor cells (MDSC) and tumor associated macrophages (TAM)(22, 23). A recent strategy to combat this resistance aims at targeting the chemotactic signals provided by PDAC cells which recruit TAMs to the tumor microenvironment. Both murine and human studies have confirmed that high macrophage infiltration is associated with worse outcome and inhibiting the population results in enhanced anti-tumor immunity(7, 8, 19). Because of the prognostic importance and need to track response to therapy, a non-invasive method to track macrophage accumulation is essential.

In this study, we tested the utility of [11C]PBR28 to track the accumulation and depletion of macrophages using a murine model of PDAC. With high affinity for the steroid transporter TSPO, [11C]PBR28 uptake has been previously demonstrated to be elevated in activated glial cells in the brain(11, 12) and in macrophages in models of rheumatoid arthritis(15), colitis(24) and aortic aneurysms(16). We hypothesized that this same strategy could be used to image activated macrophages in pancreatic cancer. To study this, tumor cells derived from a spontaneous murine PDAC were placed subcutaneously in syngeneic mice. This location allowed tumors to be measured and imaged without potential interference from surrounding organs such as the kidney or spleen. We confirmed that the PDAC cell line used had no native TSPO staining while splenocytes and purified macrophages harvested from mice had abundant expression. Levels of TSPO appeared to increase when macrophages were activated to either an M1 or M2 phenotype, consistent with prior publications(5). To

unequivocally demonstrate [11C]PBR28 uptake and distribution, autoradiography of tissues of interest resected shortly after radioisotope injection was performed. Autoradiography confirmed that [11C]PBR28 uptake is high in the kidney (positive control) and wild type tumor, and low in skeletal muscle (negative control). This behavior was confirmed by immunofluorescent staining obtained from the same tissue specimens.

To confirm that these findings were macrophage specific, a well-established model of macrophage depletion was used. The CD11b-DTR mouse is genetically altered such that myeloid cells express the diphtheria toxin making them susceptible to cell death when DT is exogenously administered. After subcutaneous tumors were established, mice received repeated doses of DT. Upon confirmation of macrophage depletion in the tumor and spleen by IHC and flow cytometry, we found decreased [11C]PBR28 uptake in tumors by autoradiography supporting our hypothesis. To test for clinical relevance, mice underwent microPET imaging after [11C]PBR28 injection and the subcutaneously placed pancreatic (wild type) tumors were readily detectable.

Alterations in the immune infiltrate are a hallmark of pancreatic cancer and is proposed to be a driver of both tumor progression and resistance to immune-mediate destruction(25). While previous efforts have focused on lymphocyte infiltration in tumors, more recent investigations have identified an important role for macrophages. A recently completed Phase 1 clinical trial of the CCR2 inhibitor PF-04136309 demonstrated efficacy in decreasing tumor associated macrophage infiltration and suggested improved tumor control(8). A Phase 3 trial is currently underway.

We have demonstrated that [11C]PBR28 can be used to track tumor associated macrophages. We therefore postulate that [11C]PBR28 PET can serve as a valuable tool for selection of suitable candidates for macrophage targeted therapies as well as for response evaluation of such therapies.

One of the limitations of TSPO use is its relative lack of specificity both do to inherent expression in kidney tissue and the abundance of macrophages in organs such as the kidney and spleen. This could be easily mitigated in human studies by co-localization and measurement of activity in the pancreas using paired cross sectional and PET images as has been established in human biodistribution studies(13).

Conclusions

The role and significance of tumor associated macrophages in pancreatic cancer has been well established. [11C]PBR28 appears to be a promising radiotracer to determine the degree of macrophage infiltration into PDAC. We therefore consider [11C]PBR28 a promising imaging biomarker to identify patients who might benefit from myeloid based immunotherapies.

References:

1. Hariharan D, Saied A, Kocher HM Analysis of mortality rates for gallbladder cancer across the world. HPB : the official journal of the International Hepato Pancreato Biliary Association 2008:10:327–331. [PubMed: 18982147]

2. Rahib L, Smith BD, Aizenberg R, Rosenzweig AB, Fleshman JM, et al. Projecting cancer incidence and deaths to 2030: the unexpected burden of thyroid, liver, and pancreas cancers in the United States. Cancer research 2014:74:29132921.

3. Gunturu KS, Rossi GR, Saif MW Immunotherapy updates in pancreatic cancer: are we there yet? Therapeutic advances in medical oncology 2013:5:81–89. [PubMed: 23323149]

4. Royal RE, Levy C, Turner K, Mathur A, Hughes M, et al. Phase 2 trial of single agent Ipilimumab (anti-CTLA-4) for locally advanced or metastatic pancreatic adenocarcinoma. Journal of immunotherapy 2010:33:828–833. [PubMed: 20842054]

5. Topalian SL, Hodi FS, Brahmer JR, Gettinger SN, Smith DC, et al. Safety, activity, and immune correlates of anti-PD-1 antibody in cancer. The New England journal of medicine 2012:366:2443–2454. [PubMed: 22658127]

6. Mitchem JB, Brennan DJ, Knolhoff BL, Belt BA, Zhu Y, et al. Targeting tumorinfiltrating macrophages decreases tumor-initiating cells, relieves immunosuppression, and improves chemotherapeutic responses. Cancer research 2013:73:1128–1141. [PubMed: 23221383]

7. Sanford DE, Belt BA, Panni RZ, Mayer A, Deshpande AD, et al. Inflammatory monocyte mobilization decreases patient survival in pancreatic cancer: a role for targeting the CCL2/CCR2 axis. Clinical cancer research : an official journal of the American Association for Cancer Research 2013:19:3404–3415. [PubMed: 23653148]

8. Nywening TM, Wang-Gillam A, Sanford DE, Belt BA, Panni RZ, et al. Targeting tumour-associated macrophages with CCR2 inhibition in combination with FOLFIRINOX in patients with borderline resectable and locally advanced pancreatic cancer: a single-centre, open-label, dose-finding, non-randomised, phase 1b trial. The Lancet. Oncology 2016:17:651–662. [PubMed: 27055731]

9. Corsi L, Geminiani E, Baraldi M Peripheral benzodiazepine receptor (PBR) new insight in cell proliferation and cell differentiation review. Current clinical pharmacology 2008:3:38–45. [PubMed: 18690876]

10. Batarseh A, Papadopoulos V Regulation of translocator protein 18 kDa (TSPO) expression in health and disease states. Molecular and cellular endocrinology 2010:327:1–12. [PubMed: 20600583]

11. Rupprecht R, Papadopoulos V, Rammes G, Baghai TC, Fan J, et al. Translocator protein (18 kDa) (TSPO) as a therapeutic target for neurological and psychiatric disorders. Nature reviews. Drug discovery 2010:9:971–988. [PubMed: 21119734]

12. Ching AS, Kuhnast B, Damont A, Roeda D, Tavitian B, et al. Current paradigm of the 18-kDa translocator protein (TSPO) as a molecular target for PET imaging in neuroinflammation and neurodegenerative diseases. Insights into imaging 2012:3:111–119. [PubMed: 22696004]

13. Brown AK, Fujita M, Fujimura Y, Liow JS, Stabin M, et al. Radiation dosimetry and biodistribution in monkey and man of 11C-PBR28: a PET radioligand to image inflammation. Journal of nuclear medicine : official publication, Society of Nuclear Medicine 2007:48:2072–2079.

14. Scarf AM, Kassiou M The translocator protein. Journal of nuclear medicine : official publication, Society of Nuclear Medicine 2011:52:677–680.

15. Shao X, Wang X, English SJ, Desmond T, Sherman PS, et al. Imaging of carrageenan-induced local inflammation and adjuvant-induced systemic arthritis with [(11)C]PBR28 PET. Nuclear medicine and biology 2013:40:906–911. [PubMed: 23891203]

16. English S, Diaz J, Shao X, Gordon D, Bevard M, et al. Utility of 18 F-FDG and 11C-PBR28 microPET for the assessment of rat aortic aneurysm inflammation. EJNMMI Res 2014:4:1–29. [PubMed: 24382020]

17. Shao X, Fawaz MV, Jang K, Scott PJ Ethanolic carbon-11 chemistry: the introduction of green radiochemistry. Appl Radiat Isot 2014:89:125–129. [PubMed: 24631743]

18. Collins MA, Bednar F, Zhang Y, Brisset JC, Galban S, et al. Oncogenic Kras is required for both the initiation and maintenance of pancreatic cancer in mice. The Journal of clinical investigation 2012:122:639–653. [PubMed: 22232209]

19. Zhang Y, Velez-Delgado A, Mathew E, Li D, Mendez FM, et al. Myeloid cells are required for PD-1/PD-L1 checkpoint activation and the establishment of an immunosuppressive environment in pancreatic cancer. Gut 2017:66:124–136. [PubMed: 27402485]

20. Hariharan D, Saied A, Kocher HM Analysis of mortality rates for pancreatic cancer across the world. HPB : the official journal of the International Hepato Pancreato Biliary Association 2008:10:58–62. [PubMed: 18695761]

21. Lucas AL, Malvezzi M, Carioli G, Negri E, La Vecchia C, et al. Global Trends in Pancreatic Cancer Mortality From 1980 Through 2013 and Predictions for 2017. Clinical gastroenterology and hepatology : the official clinical practice journal of the American Gastroenterological Association 2016:14:1452–1462 e1454.

22. Kurahara H, Shinchi H, Mataki Y, Maemura K, Noma H, et al. Significance of M2-polarized tumor-associated macrophage in pancreatic cancer. The Journal of surgical research 2011:167:e211–219. [PubMed: 19765725]

23. Allavena P, Sica A, Solinas G, Porta C, Mantovani A The inflammatory microenvironment in tumor progression: the role of tumor-associated macrophages. Critical reviews in oncology/ hematology 2008:66:1–9. [PubMed: 17913510]

24. Kurtys E, Doorduin J, Eisel UL, Dierckx RA, de Vries EF Evaluating [11C]PBR28 PET for Monitoring Gut and Brain Inflammation in a Rat Model of Chemically Induced Colitis. Mol Imaging Biol 2017:19:68–76. [PubMed: 27402092]

25. Pillarisetty VG The pancreatic cancer microenvironment: an immunologic battleground. Oncoimmunology 2014:3:e950171. [PubMed: 25610740]

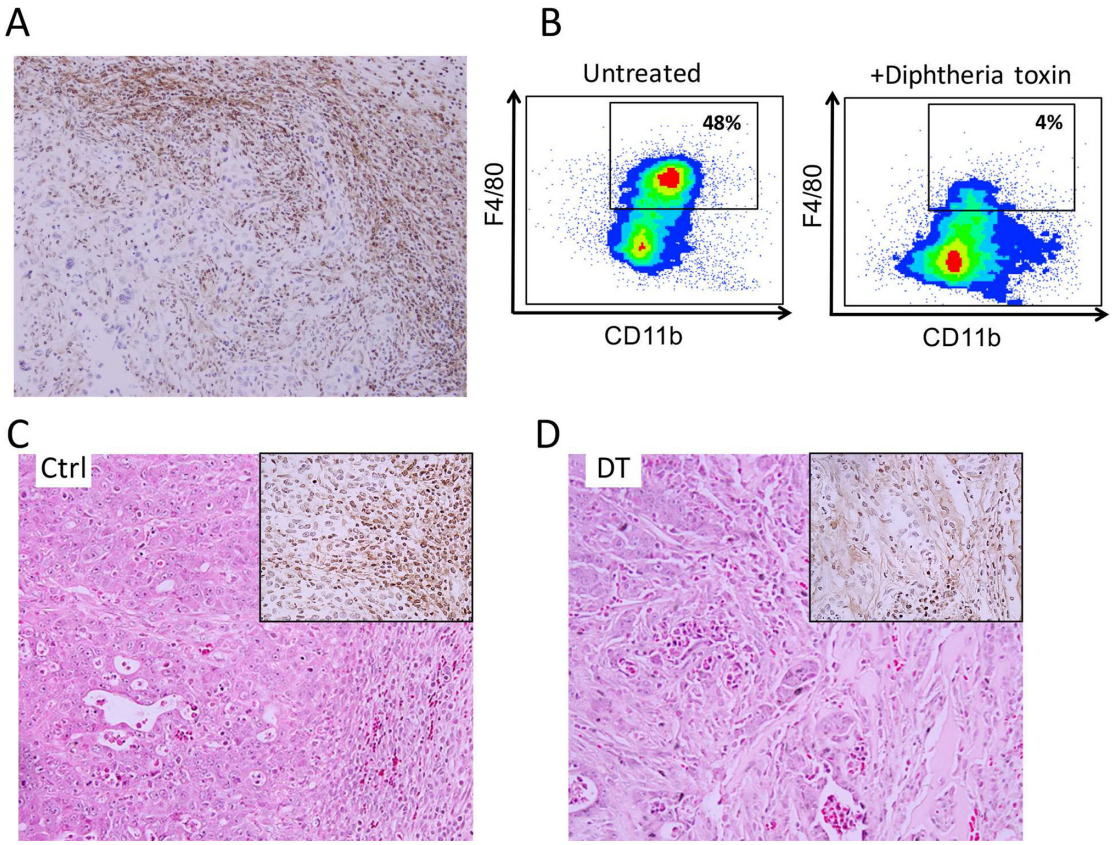

Figure 1: Tumor microenvironment of pancreatic cancer contains abundant macrophages.
Elevated macrophages are seen in the microenvironment as determined by (A) immunohistochemistry (IHC) for the macrophage marker F4/80. (B) Flow cytometry for $CD45^{+}CD3^{-}CD11b^{+}F4/80^{+}$cells confirms decrease in macrophages after diphtheria toxin treatment in CD11b-DTR mice. (C,D) Results were confirmed by IHC for F4/80.

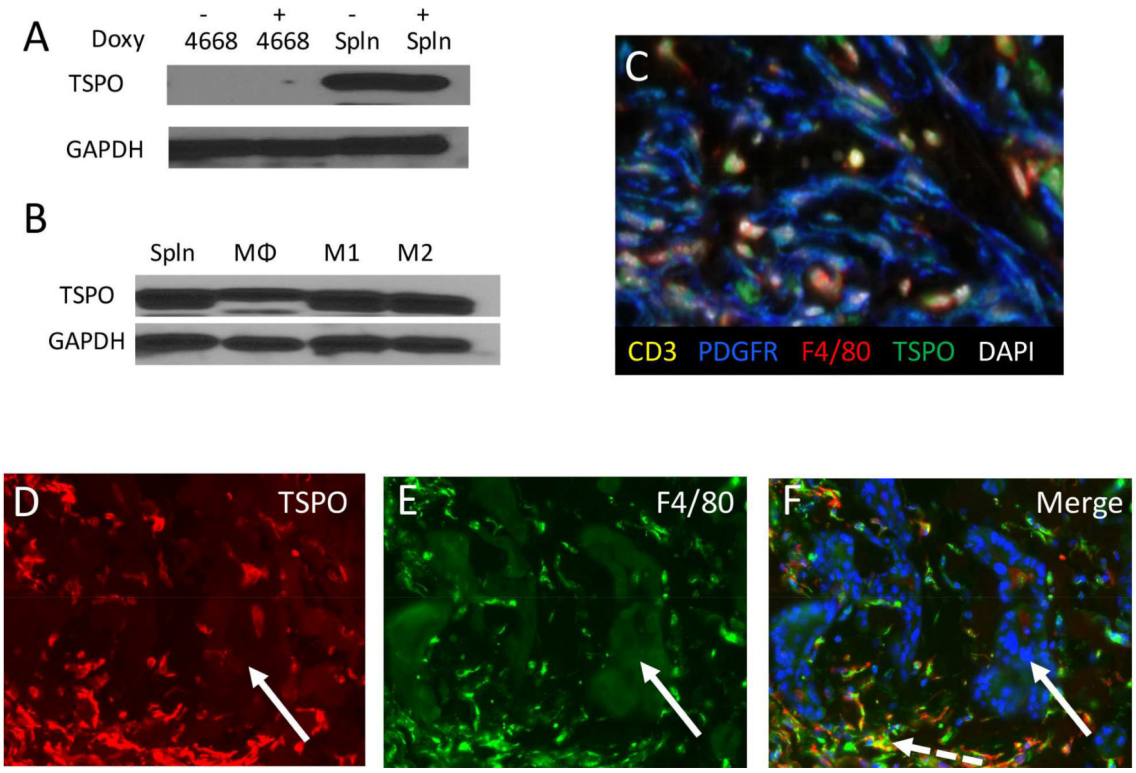

Figure 2: TSPO expression.

(A) Western blot analysis reveals lack of TSPO protein expression in the murine pancreatic cancer line 4668 with and without KRAS activation while harvested splenocytes demonstrate robust staining. (B) Activation of macrophages to an M1 or M2 phenotype results in increased TSPO expression. (C) Multiplex fluorescent imaging of the stroma identified TSPO expression (green) in macrophages ($F4/80^+$, red) but not fibroblasts ($PDGFR^+$, blue) or lymphocytes ($CD3^+$, yellow). Immunofluorescent staining of subcutaneously implanted PDAC tumors for (D) TSPO (red) and (E) F4/80 (green) and the nuclear counterstain DAPI (blue). (F) Merged images confirm both TSPO presence in macrophages (dashed white arrow) and absence in epithelial cells (solid white arrow).

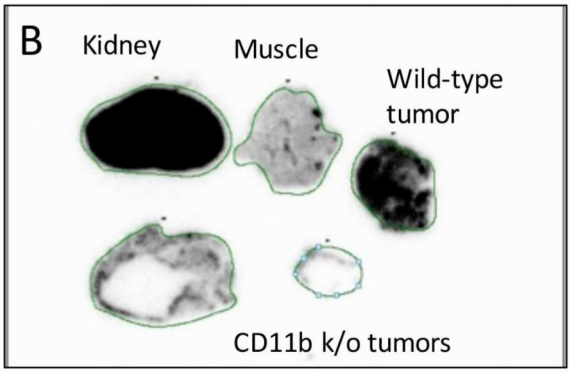

C

Mouse	Strain	Tumor-1	Tumor-2	Kidney	Muscle
1	WT	2.5	1.2	12.4	1
2	WT	3.4	3.3	38.6	1
3	WT	1.6	n/a	9.5	1
4	CD11b$^{-/-}$	0.8	n/a	12.5	1
5	CD11b$^{-/-}$	1.0	0.3	6.8	1

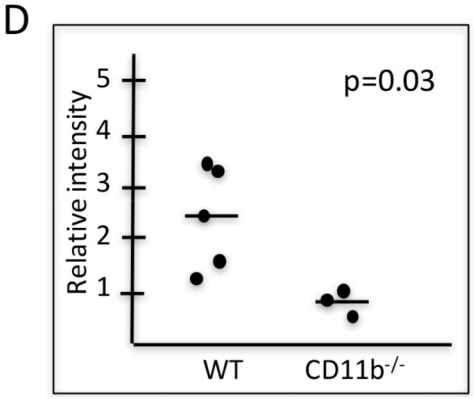

Figure 3: [11C]PBR28 radiotracer detection.

(A,B) Autoradiography performed on resected tumors and tissue confirm [11C]PBR28 radiotracer uptake in kidney (positive control) and tumors from wild type mice (n = 3 mice, 5 tumors) while little uptake is seen in muscle (negative control) and tumors for CD11b$^{-/-}$ mice (n = 2 mice, 3 tumors). (C,D) When normalized to uptake in muscle, tumors from wild type mice displayed significantly higher radiotracer uptake than those from macrophage-depleted mice.

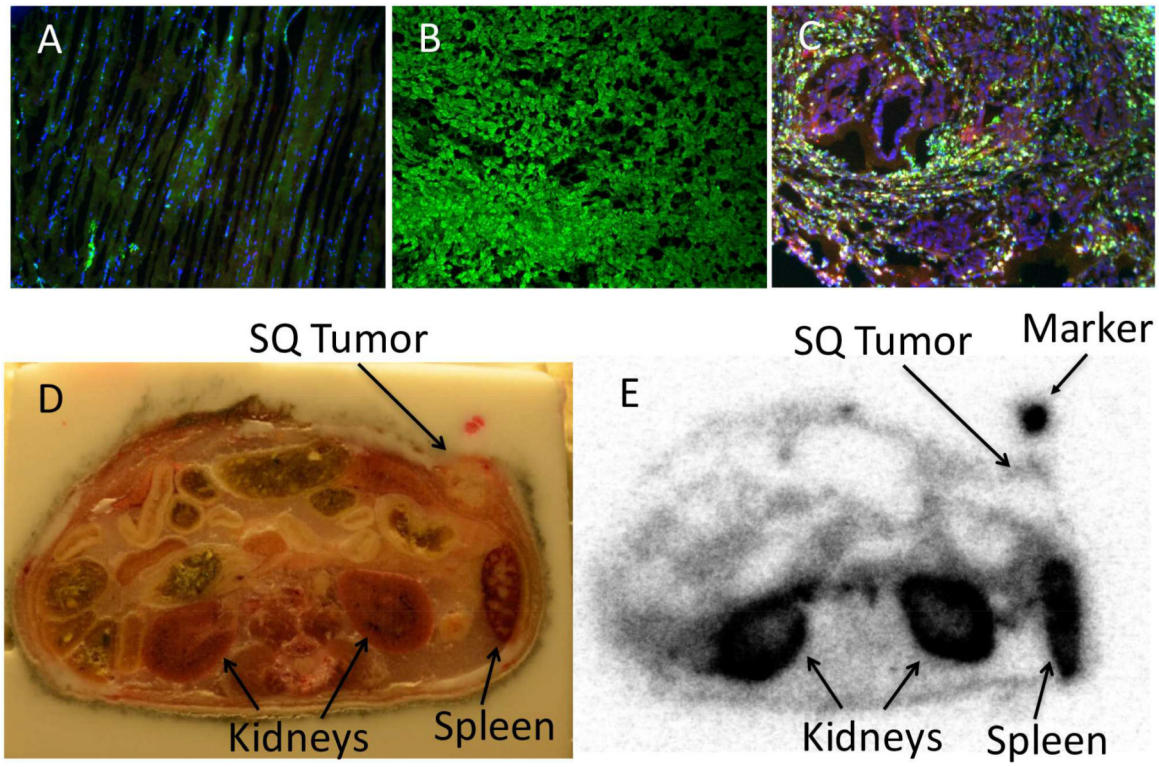

Figure 4: [11C]PBR28 localizes to TSPO positive tissues.

Immunofluorescent staining of (A) muscle, (B) kidney, and (C) pancreatic tumors for TSPO (green), F4/80 (yellow), CK19 (red) and DAPI (blue) confirmed association with radiotracer uptake. To determine if [11C]PBR28 could localize tumors in vivo, (D) whole mount sections were prepared after radiotracer administration. (E) Autoradiography confirmed the ability to localize the subcutaneous tumor (n = 3 mice, representative example shown).

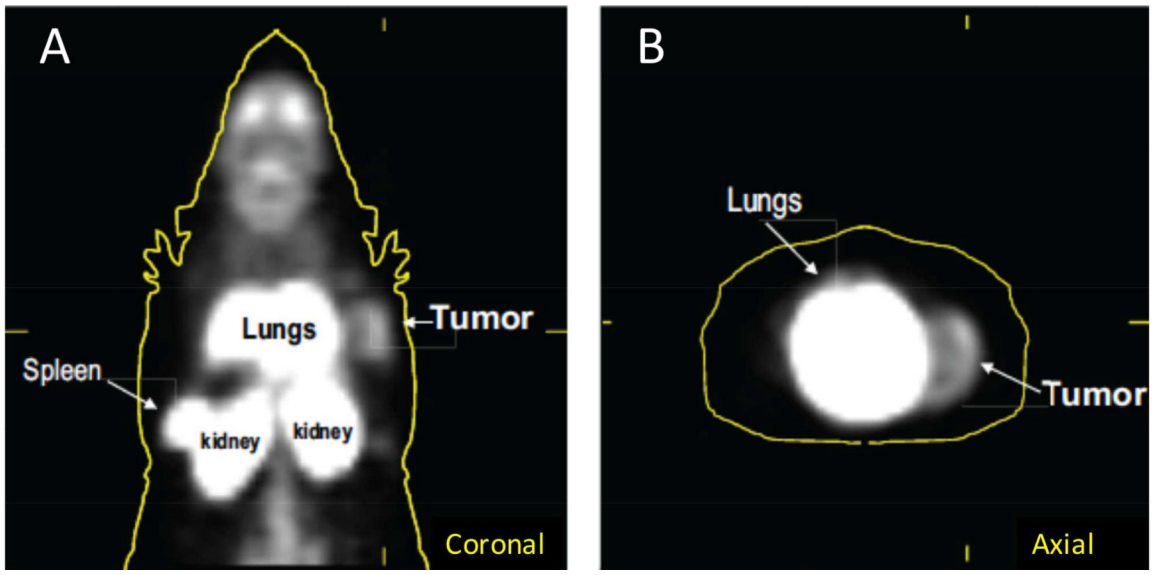

Figure 5: ***In vivo*** **[11C]PBR28 uptake.**

After [11C]PBR28 radiotracer administration mice underwent standard microPET imaging. Uptake is visible in the spleen, kidney and lungs as evident on (A) coronal and (B) axial images (n = 3 mice, representative example shown).